Journal of Environmental Chemical Engineering 10 (2022) 107748

Contents lists available at ScienceDirect

Journal of Environmental Chemical Engineering

journal homepage: www.elsevier.com/locate/jece

An investigation on pyrolysis of textile wastes: Kinetics, thermodynamics, in-situ monitoring of evolved gasses and analysis of the char residue

Gamzenur Özsin [a,b,*], Ayşe Eren Pütün [c]

[a] Bilecik Şeyh Edebali University, Faculty of Engineering, Department of Chemical Engineering, Bilecik 11210, Turkey
[b] Imperial College London, Faculty of Engineering, Department of Chemical Engineering, London SW7 2BU, UK
[c] Anadolu University, Faculty of Engineering, Department of Chemical Engineering, Eskişehir 26555, Turkey

ARTICLE INFO

Editor: Despo Kassinos

Keywords:
Textile waste
Thermogravimetric analysis
Kinetic
Gas analysis
FT-IR and MS spectroscopy

ABSTRACT

Recycling the ever-increasing industrial waste has become a pressing concern globally and pyrolysis is regarded as one of the up-and-coming techniques to recover the energy and chemical content of organic wastes. The pyrolysis of a representative industrial waste as textile waste was investigated within the scope of this study. In this way, efficient thermochemical conversion processes may be designed and optimized by creating value-added products. Different heating rates were applied to determine pyrolysis behavior using a thermogravimetric analyzer (TGA) coupled with a mass spectrometer (MS) and a Fourier transform infrared spectrometer (FT-IR). According to the obtained thermograms, the active pyrolysis region was selected for studying the kinetics, various iso-conversional methods (Friedmann, Kissinger-Akahira-Sunose; Flynn-Wall-Ozawa and Starink) were applied to the non-isothermal TG data, and the results were compared among themselves. The mean activation energy was 186.7, 185.8, 185.1, and 185.5 kJ/mol for the Friedmann, Flynn-Wall-Ozawa, Kissinger-Akahira-Sunose, and Starink models, respectively. The activation energy variation was found in good agreement among different kinetic models. The activation energy changes that were found provided a representation of the process kinetics which were described by multiple reaction schemes. All four kinetic methods were found to be applicable to forecasting the non-isothermal pyrolysis of textile wastes, although the existence of small variations in the activation energy values. Furthermore, thermodynamic parameters as enthalpy, Gibbs free energy, and entropy changes were estimated.The gasses that evolved during pyrolysis were identified by simultaneous monitoring of MS and FT-IR spectra and the temperature-dependent alteration of main volatile products were obtained. Moreover, the char residue was analyzed via ex-situ SEM-EDX and FT-IR.

1. Introduction

There is an increasing requirement for continuous economic development to reduce the consumption of finite fossil fuel reserves, to reduce the current dependency on such fossil resource reserves, and to prompt searches for alternatives. On the other hand, the massive increase in the generation of municipal and industrial wastes due to rapid industrialization and population growth has become a worldwide concern [1]. The massive consumption of energy and commodities matched with the population growth and urbanization give rise to solid waste generation that causes important threats to the environment if not disposed of or effectively recycled [2,3]. Therefore, sustainable and environment-friendly waste treatment techniques have been adopted for waste disposal. Nowadays, efforts have focused on to design and operate innovative treatment facilities that combine organic waste disposal from different origins and/or synthesis of fuels, value-added materials and chemical feedstock via sustainable green processes [4]. With this in mind, thermochemical conversion techniques such as gasification, incineration and pyrolysis seem attractive considering socio-economic and socio-environmental aspects simultaneously [5–8]. In comparison to other thermochemical conversion processes, pyrolysis is known to be one of the most flexible, cleanest and convenient methods for recycling organic wastes in terms of releasing harmful pollutants [9,10] as well as adding additional value to wastes by achieving energy recovery while promoting circular economy [11–14]. It has considerable advantages of reduction, harmlessness, stabilization, and resource recovery during waste disposal [15]. A variety of organic wastes from different origins such as agricultural wastes, plastic wastes [16–18], industrial wastes

* Corresponding author at: Bilecik Şeyh Edebali University, Faculty of Engineering, Department of Chemical Engineering, Bilecik 11210, Turkey.
E-mail addresses: g.ozsin@imperial.ac.uk, gozsin@anadolu.edu.tr (G. Özsin), aeputun@anadolu.edu.tr (A.E. Pütün).

https://doi.org/10.1016/j.jece.2022.107748
Received 14 March 2022; Received in revised form 12 April 2022; Accepted 15 April 2022
Available online 22 April 2022

[19–21] and municipal wastes [22,23] can be evaluated alone or together via pyrolysis and co-pyrolysis processes. By this way, value-added products can be produced and industrial symbiosis can be established among several industries such as food-manufacturing [24], petrochemical [25] and polymer [26] industries. In particular, a bulk quantity of industrial wastes such as textile wastes has been collected on site because of accelerated industrialization and high production rates which makes them feasible candidates for recovery via pyrolysis processes. Moreover, the fast fashion cycle gives rise to enormous production and consumption quantities of textiles and waste generation which make the textile industry one of the most polluting industries [27,28]. It is well known that the average global annual consumption of textiles has dramatically increasing which in turn indicates simultaneous accumulation of textile wastes in large quantities [29].

According to the recent industrial reports, $400 Billion worth of clothing is wasted every year and a considerable amount of textile waste is discarded into landfill. About, two thirds of the discarded materials are known to be man-made fibers that takes decades to decay. When it comes to polymer based textiles, it will take 200 years to breakdown in the landfill[30]. Unfortunately, Approximately 87% of global textile waste ends up in landfill or incineration, while over 95% of that can be reused or recycled [31,32]. In comparison to other industrial wastes, scarce attention has been devoted to the pyrolysis of textile wastes although regional production rates are colossal in developing countries like Turkey. It is known that value-added syn-gas [33,34], solid-phase products such as porous sorbents and fuel [35–37] with some high-quality liquid products [38] can be obtained from the pyrolysis of textile wastes. Especially, cellulosic fibrous materials in such textile wastes can be utilized in the production of bio-based carbonaceous materials via pyrolysis processes. For instance, Nahil and Williams [39] showed that acrylic textile waste can be used as precursor material for the preparation of activated carbon while Zheng et al. [40] performed a study on activated carbon fiber production using cotton woven waste as a precursor.

However, a deep awareness on the process of pyrolysis and the pyrolytic decomposition mechanism is imperative for better modelling approaches for pyrolysis systems. Such approaches are ultimately used in design and optimization as they provide a better perception about the pyrolytic decomposition mechanism. Since pyrolysis is the essence of most other thermochemical conversion techniques such as combustion and gasification, profound knowledge on its kinetics is critical to the assessment of the feasibility, design, and scaling of the industrial applications of other thermochemical conversion technologies [41]. The thermogravimetric analysis (TGA) technique is one of the prevailing methods of both investigating thermal events and determining kinetic parameters during thermochemical conversion since weight loss materials reflect physical and chemical structural transformation processes. However, the presence of overlapping zones on thermograms, the uncertainty about the interaction effects, and the difficulty to gain analytical precise results have limited the sole use of TGA in thermal degradation studies [42]. In recent years, there has been an expanding interest in hyphenated TGA techniques such as FT-IR and MS that are utilized for gathering further information about evolved species during pyrolysis. TGA coupled with FT-IR and MS is used to determine the pyrolytic characteristics, kinetics and evolved products of several materials [43,44]. In this study, textile waste from a local fabric manufacturing company was used as a feedstock for pyrolysis. This study aimed at the kinetic analysis of textile waste pyrolysis using different iso-conversional methods via thermogravimetry for the first time. This analysis process was also coupled with the in-situ online recording of evolved gasses using Fourier Transform-Infrared (FT-IR) and mass spectrometry (MS) since determining and appraising all potential secondary products that could be obtained from such textile wastes demands robust, selective, benign and reproducible analytical conceptualization. This thorough study can contribute a beneficial reference for the pyrolysis of textiles, which is dependent on an environmentally friendly and sustainable waste to energy conversion process.

2. Materials and Methods

2.1. Non-isothermal TGA/FT-IR experiments

Mixed waste fabric pieces were obtained from a local waste recycling company (Akkent Textile Co.) which collects and reprocess different types of textiles including cotton and polyester. Prior to thermoanalytical measurements, the wastes were mixed and ground cryogenically using a high-speed rotary mill. After the homogenization of the samples, they were sieved, and a particle size of 112 μm was used in the experiments. By performing proximate and ultimate analyses, the characteristics of the mixed fabrics were determined. The gross calorific values were calculated by the Dulong's formula as it is given in Uzun et al.[45].

The pyrolysis of the textile waste was studied with a thermo analyzer (Setaram Labsys Evo) coupled with an FT-IR spectrometer (Thermo Scientific Nicolet Iz 10) and an MS (Pfeiffer Omni Star) spectrometer. About 10 mg of the sample was evenly distributed over an Al_2O_3 crucible for good dispersion and put into the TGA furnace to prevent a possible temperature gradient in the sample and ensure the kinetic control of the process. Before heating the sample, a 30-min purging period was applied for the sample to flush out traces of air from the system. Nitrogen was supplied to the thermo analyser at a flow rate of 20 mL/min during the process to maintain the inert atmosphere in all experiments. The sample was heated from 25 °C to the final temperature of 1000 °C with different linear heating rates as 5, 10, 20 and 40 °C/min.

The evolved gases that formed during the TGA measurements were carried to both FT-IR and MS devices simultaneously. Transfer lines were kept at constant temperatures to prevent the condensation of volatiles or adsorption on the transfer lines because a broad range of volatile gases such as vapours of some organic compounds was expected. For detecting volatiles, FT-IR measurements were made in the continuous scan mode, and IR spectra were recorded in the range of 400–4000 cm^{-1}. Volatiles were also scanned simultaneously for the selected m/z values during the MS analysis. The MS device was operated under a vacuum, and the in-situ detection of the intensity of the characteristic fragment ion of the associated gasses according to its mass to charge ratio (m/z) was performed. An SEM-type detector was used for multiple ion detection (MID) scanning and the signals of the mass/charge ratios (m/z) for the targeted compounds were recorded. The analyses were performed in triplicates to ensure precision in the results.

The fixed-bed pyrolysis experiments were performed to identify the product yields of solid, liquid and gaseous products at 500 ℃. The separation of phases after the reaction was followed the same procedure as it was described in our previous paper [46].

2.2. Calculation of kinetic parameters

Thermogravimetric analyzer records mass change of the sample as a function of time and temperature in a specified atmosphere and thereby it used to observe the thermal conversion of materials. The obtained data from isothermal or non-isothermal thermogravimetry can also give insight into the kinetic parameters of the process. The isothermal and non-isothermal techniques differ depending on the data collection method that includes monitoring change in the weight loss of the sample with respect to time in constant temperature or linear temperature change [47]. The data gathered data from non-isothermal TGA experiments at different heating rates can be used along with kinetic approach to support pyrolytic degradation behaviors of complex materials. However, isothermal experiments are hard to consistently manage because of the presence of non-isothermal heating time between the heating element and the sample during analysis.

The basic rate equation of solid-state thermal decomposition processes assume that the conversion rate is proportional to the concen-

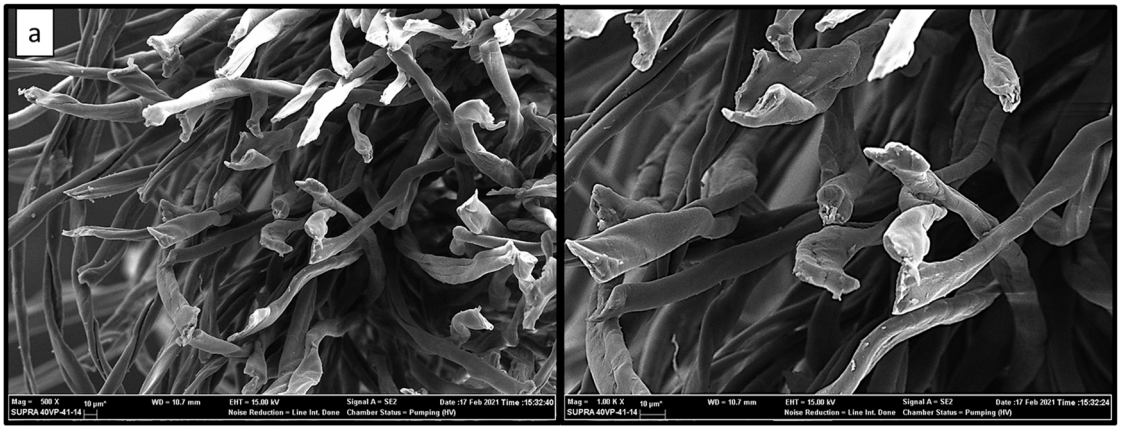

Ultimate Analysis (as-received basis)	
C (%)	45.60
H (%)	6.45
N (%)	0.56
O* (%)	47.39
H/C	0.68
O/C	0.78
HHV (MJ/kg)	16.18
Proximate Analysis (as-received basis)	
Moisture (%)	3.28
Ash (%)	2.46
Volatiles (%)	62.42
Fixed C* (%)	31.84

*From difference

Fig. 1. Characteristics of as-received textile waste. [(SEM micrographs (a), FT-IR spectrum (b), ultimate analysis and proximate analysis table (c)].

tration of reactant and dependent on temperature. In the non-isothermal experiments, the sample weight is continuously measured as a function of time, while the reaction proceeds for a fixed heating rate, β (K/min). The kinetic equation non-isothermal thermal degradation reaction is given by the rate of change of conversion with time and is represented as dα/dt. At a linear temperature heating rate, two different independent functions, namely temperature function (k(T)) and fractional conversion function (f(α)) characterizes kinetic expression as given in Eq. 1:

$$\frac{d\alpha}{dt} = \beta\frac{d\alpha}{dT} = k(\mathrm{T})f(\alpha) \tag{1}$$

The dependency of the rate constant, k, on temperature is described by Arrhenius equation:

$$k(T) = Aexp\left(-\frac{E_a}{RT}\right) \tag{2}$$

where E_a is the activation energy, A the pre-exponential factor and R the gas constant.

By merging Eqs. (1) and (2), the reaction rate can be given in the form:

$$\beta\frac{d\alpha}{dT} = A\exp\left(-\frac{E_a}{RT}\right)f(\alpha) \tag{3}$$

Moreover, fractional conversion is written by:

$$\alpha = \frac{w_o - w_t}{w_o - w_f} \tag{4}$$

where; w_o, w_t and w_f are sample mass which presented at initial, arbitrary, and final times respectively.

Eq.(3) can also be integrated into,

$$\int_0^\alpha \frac{d\alpha}{f(\alpha)} = g(\alpha) = \frac{A}{\beta}\int_{To}^{T}\exp\left(-\frac{E_a}{RT}\right)dT \equiv \frac{AE_a}{\beta R}p(u) \tag{5}$$

g(α) and p(u) are known as the integrated form of fractional conversion function f(α) and temperature integral, respectively. The solution of p(u) can be obtained by using different approaches which utilizes different mathematical approximations such as Doyle [48], Agrawal-Sivasubramanian [49] and Senum–Yang [50].

According to the assuming reaction mechanisms, there exits two possible approaches in kinetic analysis as iso-conversional (model-free) and model-fitting (or model-based). The iso-conversional method was implemented herein to predict the kinetic parameters using heating as a function of conversion degree which depicts the progress of the process from initiation to completion. These iso-conversional methods are known to be appropriate for figuring out the kinetic parameters of complex thermal conversion reactions which can be roughly separated into two main categories as integral or differential methods. In this study, we have targeted different iso-conversional methods, namely Friedmann, Flynn-Wall-Ozawa (FWO), Kissinger-Akahira-Sunose (KAS) and Starink to determine the activation energy. Eqs. 6–9 shows the linearized forms of the kinetic models which were used during the iso-conversional kinetic analysis.

$$\ln\left(\beta\frac{d\alpha}{dT}\right) = \ln A + \ln f(\alpha) - \frac{E_a}{RT}(\text{for Friedman}) \tag{6}$$

$$\ln\beta = \ln\frac{AE_a}{Rg(\alpha)} - 5.331 - 1.052\frac{E_a}{RT}(\text{for FWO}) \tag{7}$$

$$\ln\left(\frac{\beta}{T^2}\right) = \ln\left(\frac{AR}{E_a g(\alpha)}\right) - \frac{E_a}{RT}(\text{for KAS}) \tag{8}$$

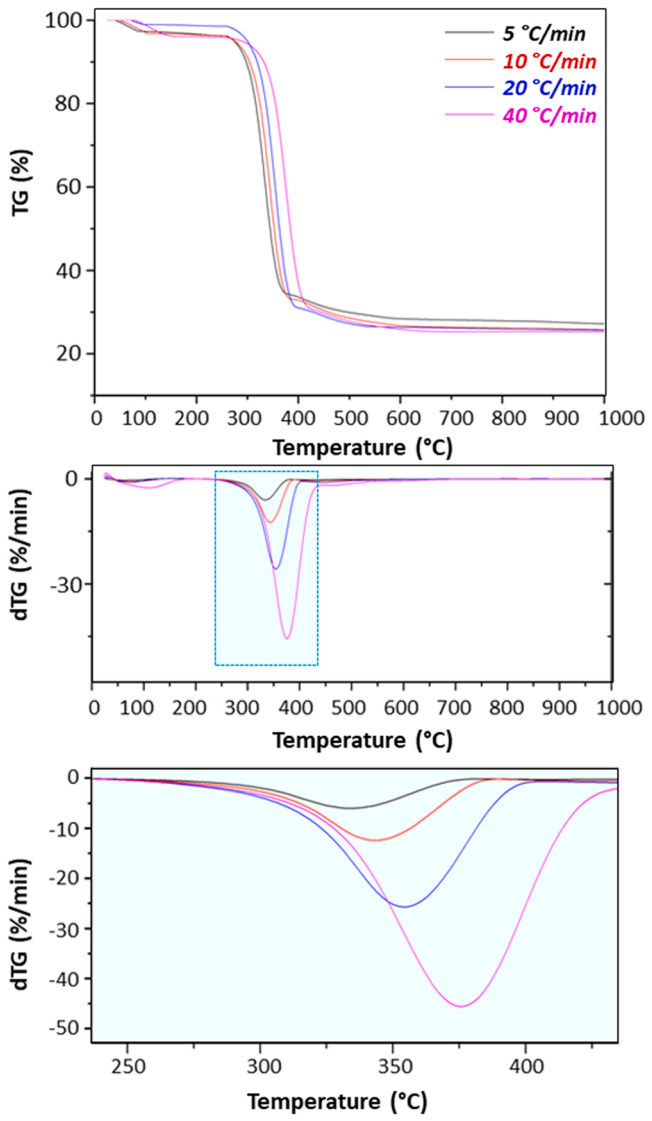

Fig. 2. TG and dTG curves of textile waste at the different heating rates.

$$\ln\left(\frac{\beta}{T^{1.8}}\right) = C_s - 1.0037\frac{E_a}{RT}\,(\text{for Starink}) \tag{9}$$

The thermodynamic parameters of the pyrolysis process, including enthalpy change (ΔH), Gibbs free energy change (ΔG), and entropy change (ΔS), were determined using Eyring method [51,52] by the help of the equations which were given below:

$$\Delta H = E_a - RT \tag{10}$$

$$\Delta G = E_a + RT_m \ln\left(\frac{K_B T_m}{hA}\right) \tag{11}$$

$$\Delta S = \frac{\Delta H - \Delta G}{T_m} \tag{12}$$

Here, K_B is Boltzmann constant (1.381 $\times 10^{-23}$ J/ K), h is the Plank constant (6.626 $\times 10^{-34}$ J. s) and T_m is the maximum temperature peak observed from the dTG curve.

3. Results and Discussion

3.1. Compositional analysis of the textile waste

It is known that the physicochemical characteristics of feedstock, play an important role in the choice of convenient thermochemical conversion techniques [53]. In general, mixed wastes of the industries tend to be more reactive than conventional fuels due to their structural characteristics, and a complete understanding of the characteristics of such wastes is required for the analysis before pyrolysis. Therefore, in this study, the composition and structure of textile waste were analyzed in detail prior to the pyrolysis experiments. Fig. 1 shows the SEM micrographs, and FT-IR spectrum together with ultimate and proximate analyses of the textile waste on an as-received basis. As seen in the SEM micrographs, the morphology of the waste was observed with magnifications of 500 and 1000X in order to determine topological changes during pyrolytic decomposition. The SEM micrographs displayed an unsmooth, non-porous, and partially disrupted surface morphology.

To verify the functional groups, present in the textile waste, FT-IR spectroscopy was performed, and the obtained spectrum is also shown in Fig. 1. As it can be seen in the spectrum, an intense peak around 3500 cm^{-1} corresponded to O-H stretching due to the moisture of the waste. Moreover, the O-H bending vibration of absorbed water was observable around 1640 cm^{-1}. Around 1240 cm^{-1}, 1090 cm^{-1} and 722 cm^{-1}, peaks were observed and assigned to the asymmetric aromatic ester stretching, C-O-C stretching and aromatic out-of-plane C-H vibration of polyester [54]. The peak at 2900 cm^{-1} indicated the C-H stretching vibration of alkyl groups, and the location of the strong band between 1310 and 1250 was assigned to the C-O stretching of the aromatic ester structure. Moreover, several bands between 1430 and 1315 were attributed to the single -CH_2 scissoring, C-H asymmetric deformation, and single -OH bending vibration of the cellulosic structure [38] that was present in the textile waste.

Ultimate and proximate analysis indicates the potential use of waste materials in pyrolysis processes. As seen in the finding shown in Fig. 1, the as-received textile waste had higher contents of C and O. The oxygen in the textile waste (47.39 wt%) was more abundant than carbon (45.60 wt%) and hydrogen (6.45 wt%). In addition, high volatile (62.42 wt%) and fixed carbon (31.84 wt%) were detected in the structure, while minor quantities of moisture (3.28 wt%) and ash (2.46 wt%) were present. High ash content is considered a problem during thermochemical conversion processes because it can cause fouling or aggregation, and result in some disposal problems, reduced energy conversion rates and ultimately increased processing costs [55]. Fixed carbon indicates the portion of the waste that must be burned in a solid-state, and has information on equipment selection since it reveals the caking properties of the material. Besides, the volatile matter concentration of the material is important for the feasibility and product distribution of pyrolysis. A relatively high volatile matter content indicates that the textile waste can be ideally converted to pyrolytic products with a high amount of gas and liquid products. In this study, the higher heating value (HHV) of the textile waste was determined from the Dulong formula according to the elemental analysis results given in Fig. 1 as 16.18 kJ/ kg. In order to characterize the degree of carbonization of the as-received material, the H/C and O/C ratios of the textile wastes are also reported in the figure as 0.68 and 0.78, respectively.

3.2. Thermogravimetric analysis and effect of heating rate

In order to extensively perceive the pyrolysis process of the textile waste, thermogravimetric analyses (TGAs) were carried out under a nitrogen atmosphere, and the effects of the heating rate were determined from the shape of the resultant thermograms. According to TG and dTG thermograms shown in Fig. 2, there was an observable shift towards a higher decomposition temperature when the heating rate was increased. The lateral shift of the shoulders and peaks can be attributed

Table 1
Characteristic pyrolysis temperatures for textile waste.

β (°C/min)	T_i (°C)	Tp (°C)	T_f (°C)	R_p (%/min.mg)
5	225.1	332.9	414.2	0.56
10	239.3	341.7	424.8	1.02
20	242.3	351.8	438.3	2.51
40	270.0	370.9	453.8	3.64

T_i is the initial active pyrolysis temperature.
Tp is the peak temperatures in active pyrolysis zone.
T_f is the terminal active pyrolysis temperature.
Rp is the pyrolysis reactivity.

to the thermal lag effect during non-isothermal experiments due to the combined effects of heat transfer and mass transfer. It is well known that a variation of the heat flow rate at the inner parts of samples is caused by different heating rates. A relatively lower heating rate can result in better heat transfer from the surface to the core of the sample, while the heat distribution can decline, and the heat transfer efficiency is reduced at higher heating rates. In general, as the heating rate increases, the peaks in dTG curves become broader. This thermal hysteresis is also related to heat transfer efficiency, which may delay the decomposition of the inner regions of the sample [56,57]. Therefore, an appreciable time is taken by the gas used in the purging process to maintain the equilibrium with the temperature of the sample in the case of higher heating rates, and hence a large amount of instantaneous energy is transferred to the sample. On the other hand, the timescale is shortened considerably at low heating rates. Thus, the temperature corresponding to the salient transformation of the different fractions in the sample at higher heating rates is increased [58]. For the heating rates of 5, 10, 20, and 40 °C/min, the peak maxima were observed at 332.9, 341.7, 351.8, and 370.9 °C, respectively as it can be seen from the Table 1. The reactivity values of pyrolysis changed from 0.56% to 3.64%/min.mg due to increasing heating rate from 5°C/min to 40°C/min. The results showed that the pyrolysis of the textile wastes commenced at temperatures above 225 °C. The thermal degradation process of textile can be divided into two main stages during heating in a nitrogen atmosphere. The first stage is characterized by slight weight loss which can be attributed to the moisture content of the sample. The next stage is the decomposition stage where the maximum weight loss occurs. After this second stage, a slight weight loss is also observable, which is related to the small-scale decomposition reactions of carbonaceous fractions. Based on the integrated dTG curves obtained in this study, the analysis of the kinetics of the main pyrolysis stage was carried out and is described in the following sections.

3.3. Kinetic analysis

To progress in the validation of realistic models for the design and optimization of pyrolysis processes on an industrial scale, obtaining kinetic data under realistic operation conditions is extremely important [59]. Fig. 3 shows the Friedman plots used for determining the activation energies (Fig. 3.a) and the activation energy values against the conversion degree by different iso-conversional methods (Fig. 3.b). Different models including the Starink, KAS, and FWO were implemented on the same experimental data used in the Friedman model analysis, since determining activation energy values by running other models with different approaches provides better information on the estimation and trend of the activation energy. The numerical values of the activation energies with their regression coefficients as the result of one-way analysis of variance (ANOVA) are given in Table 2. All the results of each kinetic model were expressed as the standard deviation (SD). Moreover, the fit model declared square correlation coefficients

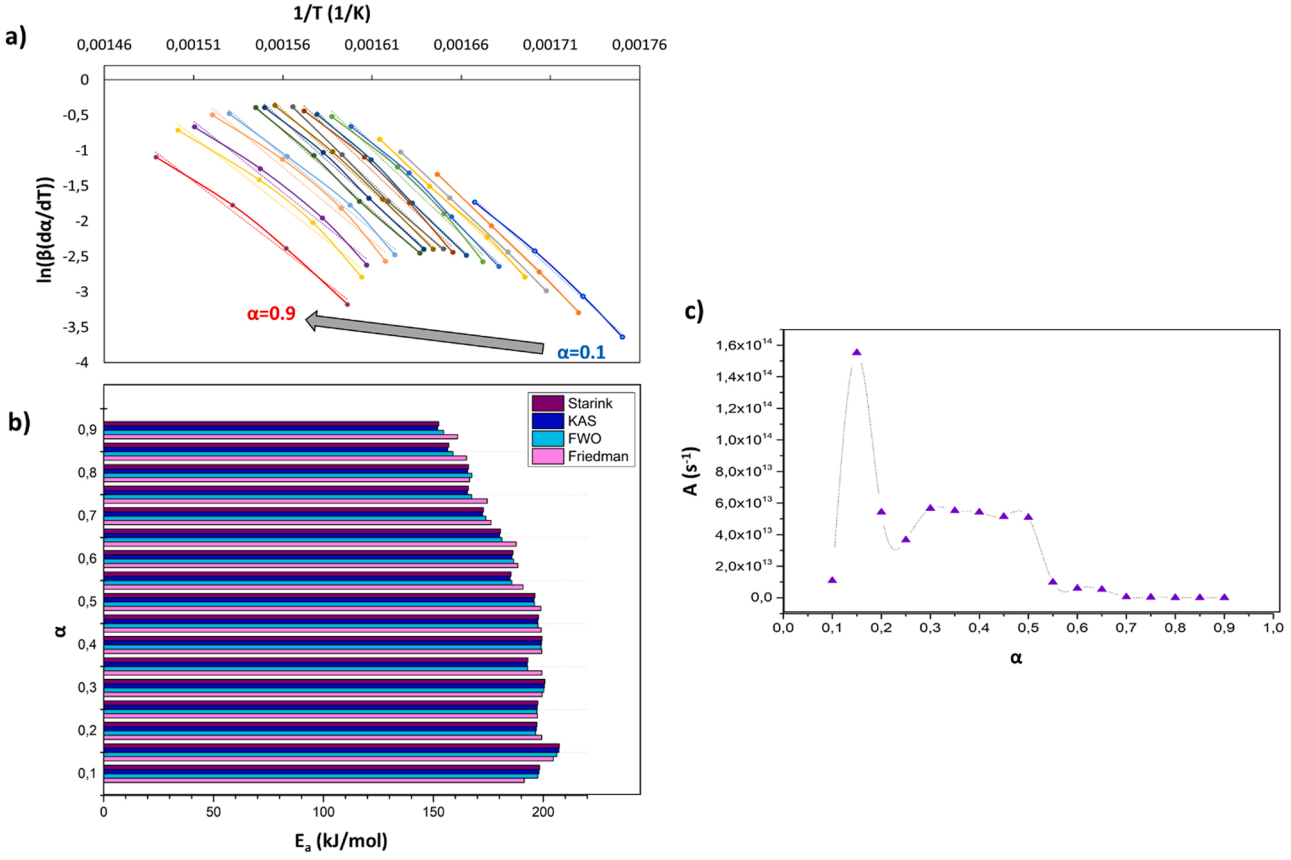

Fig. 3. Friedman plots (a), activation energy variation with conversion degree (b) and pre-exponential factor variation with conversion degree (c) for textile waste pyrolysis.

Table 2
Activation energy (kj.mol-1) with respect to conversion degree for pyrolysis of textile waste.

	Friedman		FWO		KAS		Starink		aA (s^{-1})	Compensation plot & equation
α	**E_a (kj. mol^{-1})**	**R^2**	**E_a (kj. mol^{-1})**	**R^2**	**E_a (kj. mol^{-1})**	**R^2**	**E_a (kj. mol^{-1})**	**R^2**		
0.10	191.3	0.9969	197.5	0.9911	198.1	0.9901	198.3	0.9902	1.09×10^{13}	
0.15	204.5	0.9997	206.2	0.9952	207.1	0.9947	207.3	0.9947	1.55×10^{14}	
0.20	199.3	0.9997	196.6	0.9945	196.8	0.9939	197.1	0.9940	5.42×10^{13}	
0.25	197.3	0.9988	197.1	0.9938	197.2	0.9932	197.5	0.9932	3.67×10^{13}	
0.30	199.5	0.9955	200.2	0.9956	200.5	0.9951	200.7	0.9951	5.66×10^{13}	
0.35	199.4	0.9883	192.9	0.9853	192.7	0.9836	193.0	0.9838	5.52×10^{13}	
0.40	199.3	0.9978	199.0	0.9972	199.1	0.9970	199.4	0.9970	5.42×10^{13}	
0.45	199.0	0.9912	197.6	0.9933	197.5	0.9925	197.8	0.9926	5.15×10^{13}	
0.50	199.0	0.9990	196.0	0.9987	195.9	0.9986	196.2	0.9986	5.09×10^{13}	
0.55	190.8	0.9976	185.7	0.9989	184.9	0.9987	185.3	0.9987	9.81×10^{12}	
0.60	188.4	0.9970	186.5	0.9980	185.8	0.9978	186.1	0.9978	6.06×10^{12}	
0.65	187.7	0.9989	181.2	0.9974	180.1	0.9971	180.5	0.9971	5.24×10^{12}	
0.70	176.2	0.9917	173.9	0.9956	172.3	0.9950	172.8	0.9950	5.22×10^{11}	
0.75	174.5	0.9808	167.4	0.9900	165.5	0.9885	165.9	0.9887	3.72×10^{11}	
0.80	166.5	0.9883	167.6	0.9926	165.6	0.9916	166.1	0.9917	7.40×10^{10}	
0.85	165.0	0.9802	158.9	0.9843	156.5	0.9820	157.0	0.9822	5.53×10^{10}	
0.90	161.0	0.9918	154.7	0.9945	151.9	0.9936	152.5	0.9937	2.44×10^{10}	
x^{-}	**188.2**	**0.9937**	**185.8**	**0.9939**	**185.1**	**0.9936**	**185.5**	**0.9932**	**3.22×10^{13}**	
SD	**14.1**		**15.8**		**16.9**		**16.8**			

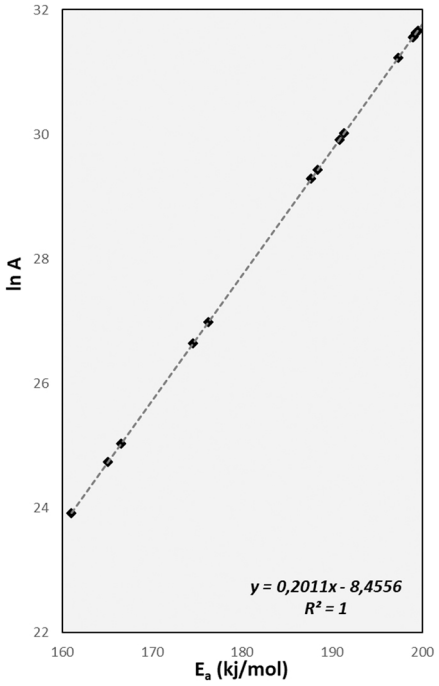

x^{-}: Average value.
SD: Standard deviation.
[a] Based on Friedman iso-conversional method.

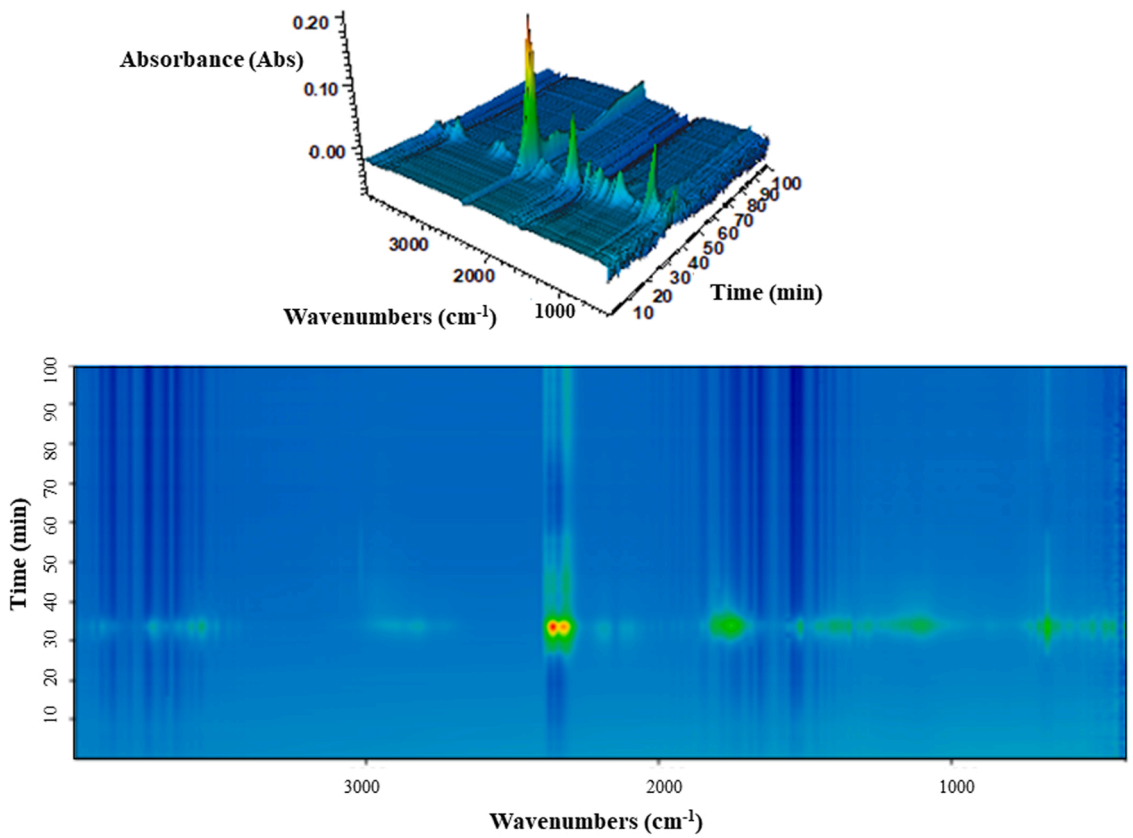

Fig. 4. 2-D and 3-D FT-IR spectra of textile pyrolysis (β = 10 °C/min).

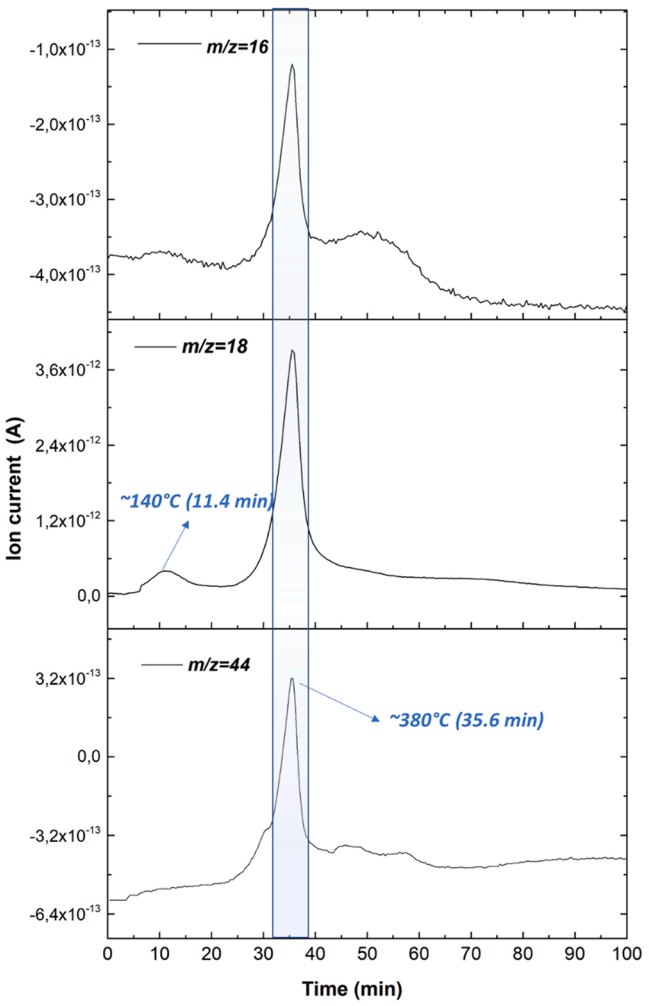

Fig. 5. Single ion current curves monitored using MS during textile waste pyrolysis (β = 10 °C/min).

(R^2) of 0.9937, 0.9939, 0.9936, and 0.9932 were harmonized with the statistical model for Friedman, FWO, KAS and Starink, respectively. The correlation coefficients at the active pyrolysis stage indicated well-fitting results. According to the results p-value that is greater than 0.05 (0.94498), as a result, four models have not significantly different in terms of activation energy.

When the activation energies along the entire conversion range were analyzed to understand the mechanism behind the textile waste pyrolysis process, it was concluded that the values with respect to the conversion degree tended to change. It is generally believed to be convenient to express the continuing pyrolytic degradation and activation energy barriers once the initial reaction commences and when the concentration of inorganics is lower than the volatile carbon content [60]. In this study, conversion degrees below 0.10 and above 0.90 were considered to estimate the kinetics of the process. According to the data, for the conversion range of 0.10–0.90, the activation energy values were found to be between 161.0 and 204.5 kj/mol using the Friedman model.

The maximum activation energy was observed at the conversion degree of 0.15 while the minimum value was at the conversion degree of 0.90 via the Friedman model. The initial activation energy was observed to be low up to a certain point which was related to the breakage of a few weak linkages and elimination of volatiles from the textile waste because all strong bonds are not likely to crack at the initial stage of the pyrolytic degradation process. Therefore, more energy is necessary for breaking these strong bonds. A slightly higher value of activation energy was determined for the initial thermal decomposition segment up to approximately the mid-point, and this slightly higher value of activation energy may be due to the presence of surface-deposited volatiles which requires more energy to drive away[61]. Since the activation energy value indicates the minimum energy demand to launch the reaction, a lower activation energy value means that the sample has a higher probability is to react sooner. On the contrary, higher activation energy values indicate the better the stability of the sample [62–65]. Therefore, the difficulty of pyrolytic reactions of the textile waste sample can be derived from the activation energy values throughout the entire degradation zone. As the pyrolytic reaction commences at the initial stages of degradation, the activation energy tends to increase at first, which shows that the degradation reaction becomes increasingly difficult at the initiation stage.

The activation energies determined from all studied methods exhibited remarkably similar fluctuation behaviors, and the numerical values obtained for the activation energy were analogous. It may be considerably difficult to obtain the convergence solution while using single-stage thermal decomposition reactions to conduct kinetic modeling due to the complex composition of textile wastes. In other words, the change in the activation energy with the conversion degree could be attributed to the degradation of different structural components [66] which resulted in fluctuations in the numerical values of the activation energy. The activation energy values estimated using the Friedman, FWO, KAS, and Starink methods also showed excellent agreement with each other; and with only a slight deviation. Moderate deviations allow determining the kinetic parameters of processes with minimal errors. For the sake of simplicity, the activation energy values calculated by using four different kinetic models were almost the same as each other with some small deviations. The small differences in activation energies are caused due to the approximations and calculations used to solve temperature integral for the derivation of the iso-conversional model equations. Based on the overall average regression coefficient values of the kinetic models explored, the experimental data better fitted with the FWO model which uses Doyle's approximation for mathematical formulation. On the other hand, Friedman, KAS, and Starink models also showed satisfying results with high regression.

In this study, the Friedman method was used in the further calculations to obtain a pre-exponential model after the interpretation of the activation energy since this method is advantageous as it does not use approximations and can be applied to any temperature program [67]. The frequency factor calculated using the Friedman equation ranged from 2.44×10^{10} to 1.55×10^{14} s^{-1}, and its variation with the conversion degree was similar to that observed in the case of the activation energy. The mean value of the pre-exponential factor was 3.22×10^{13} s^{-1}. In chemical kinetics, pre-exponential factors that are greater than 10^9 s^{-1}, are accepted to be related to a highly reactive system with a simple complex [68]. All estimated values of the pre-exponential factor over the entire degradation range were greater than 10^9 s^{-1}, implying that the complexes of the pyrolysis reaction could be transferred on the surface freely [69]. It is also well-known that a wide range of the pre-exponential values implies the alteration of the reaction chemistry and product formation with respect to the conversion degree, since it indicates the number of molecular collisions required for the reaction to occur[70,71]. Moreover, a high-level linear relationship between the activation energy and the pre-exponential factor in its natural logarithmic form (lnA) was confirmed with a high correlation coefficient of unity as demonstrated in Table 1. The observation of the compensation effect during textile waste degradation substantiates the suggestion that the analysis was reasonably able to deliver representative pre-exponential factors.

3.4. *In-situ evolved gas analysis*

The TGA/FT-IR technique is able to detect the main decomposition products based on their functional groups and the presence of covalent bonding [72]. This analysis allows to identify the removal of the

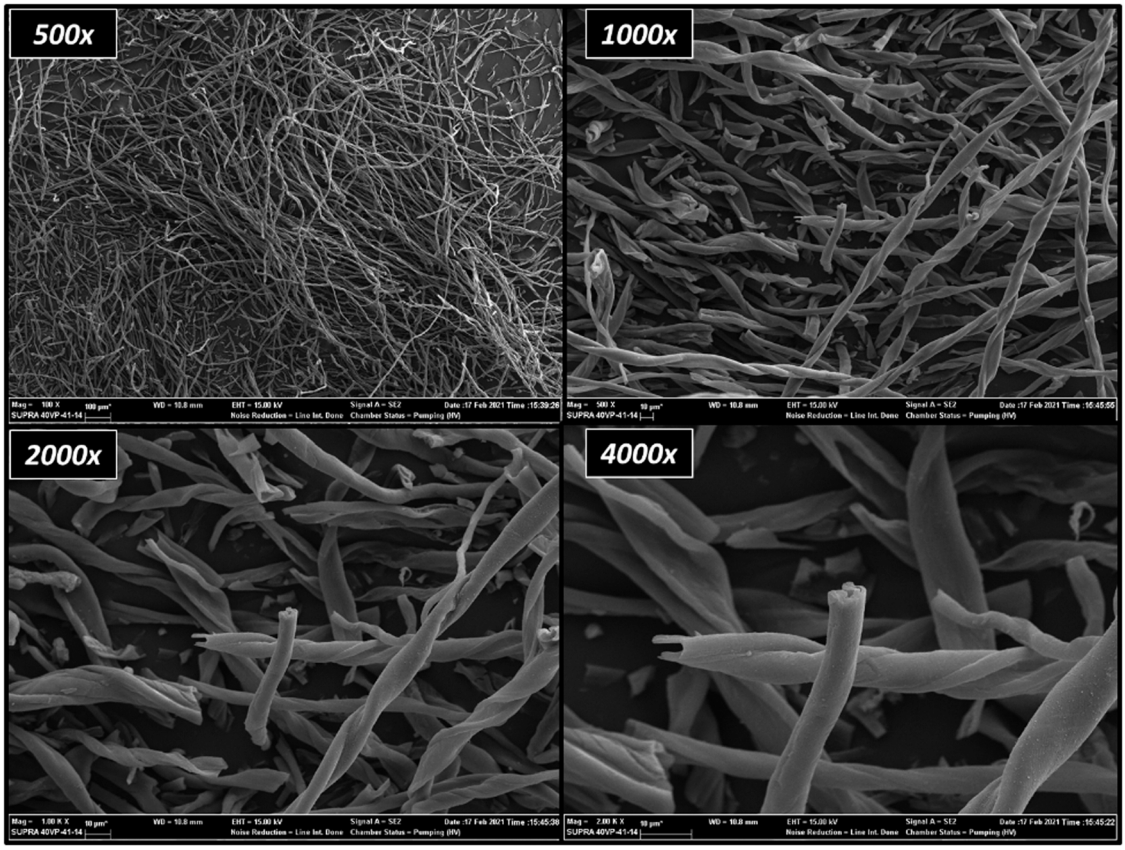

Fig. 6. SEM micrographs of char residue of textile waste.

functional groups and permanent gases during heating in real-time. Simultaneous FT-IR spectra were obtained to identify the functional groups of the active pyrolysis stage of the textile waste as shown in Fig. 4. As seen in the 2D and 3D spectra several peaks corresponding to distinct functional groups were obtained. The complexity of such spectra is an expected result of the interactions of the waste components of textiles and free radicals forming during thermal degradation. The intense gas evolution region of textile waste pyrolysis was dominated by the characteristic peak of C=O vibration. The CO_2 stretching vibrations between 2250 and 2500 cm^{-1} and the bending vibrations between 580 and 730 cm^{-1} were due to the decarboxylation reactions during the scission of the polymeric chain including intramolecular or intermolecular exchanges. The bands in the regime between 2850 and 3030 cm^{-1} belonged to the C-H stretching vibrations of light hydrocarbons. The slight O-H peak between 3100 and 3500 cm^{-1} was a characteristic indicator of H_2O as a result of the dehydration reactions that occurred during pyrolytic degradation. The absorbance peak between 2000 and 2250 cm^{-1} showed the presence of CO due to the decarbonylation reactions of pyrolysis.

Fig. 5 shows the in-situ monitoring of the evolved gaseous emissions using the MS method which offers comparative analysis with FT-IR. Signals for the ion current values for various mass numbers corresponding to the expected volatiles were collected throughout each experiment after scanning mass to charge (m/z) ratios. As a consecutive effort, the analysis was focused specifically on CH_4, H_2O, and CO_2. Mass numbers were chosen based on known fragmentation patterns, as 16, (CH_4), 18, (H_2O), and 44(CO_2), and this way, the aforementioned formation profiles were discussed with respect to the initial, maximum, and final formation temperatures. CO evolution during pyrolysis was not monitored by the MS device since the m/z ratio of the carrier gas (N_2) hinders the precise detection of CO.

It is noted that the major gas evolution that was measured for CO_2 between 260 °C (at 23.6 min) and 462 °C (at 43.7 min) with a peak at 380 °C (35.6 min). A similar peak temperature of CH_4 release was observed during the pyrolytic degradation of the textile waste at a heating rate of 10 °C/min. CH_4 evolution is known to be a result of the decomposition of the methoxy group (-OCH_3) or removal of the methyl (-CH_3) or methylene (-CH_3-) constituents [73]. Both CO_2 and CH_4 featured a sharp peak around 380 °C (35.6 min). Unlike CH_4 evolution, fragments in the evolution of CO_2 indicated several stepwise decarboxylation reactions which continued at the higher temperatures, while the CH_4 was formed within a single stage. Moreover, H_2O had a major evolution within the 265–490 °C (24.1–46.5 min) range with a maximum at 380 °C (35.6 min), while a slight evolution peak of it extended from 90° to 182°C (6.5–15.7 min). This means that, by the formation of water during pyrolysis, the dehydration reactions resulted in a defined sharp peak, while inherent water evaporation in the waste occurred at a lower temperature which was associated with the intensity of the low signal.

3.5. Analysis of the char residue

The characteristics of the raw textile waste prior to the pyrolysis and char samples in the specified conditions are presented together with kinetic data for easy interpretation of the changes that occurred during thermal decomposition. The analysis of the char residue is concerned with the observed microstructure and investigation of the elemental composition together with the existing functional groups. The average dry and ash-free basis yield of char residue at the end of the active pyrolysis zone was found as 29.7 wt% during 10 ℃/min experiments, while tar, water and gas products were 36.3, 5.9 and 28.1 wt% respectively.

To better interpret the physicochemical changes of the textile waste during pyrolytic degradation, the results from the SEM-EDX analysis of

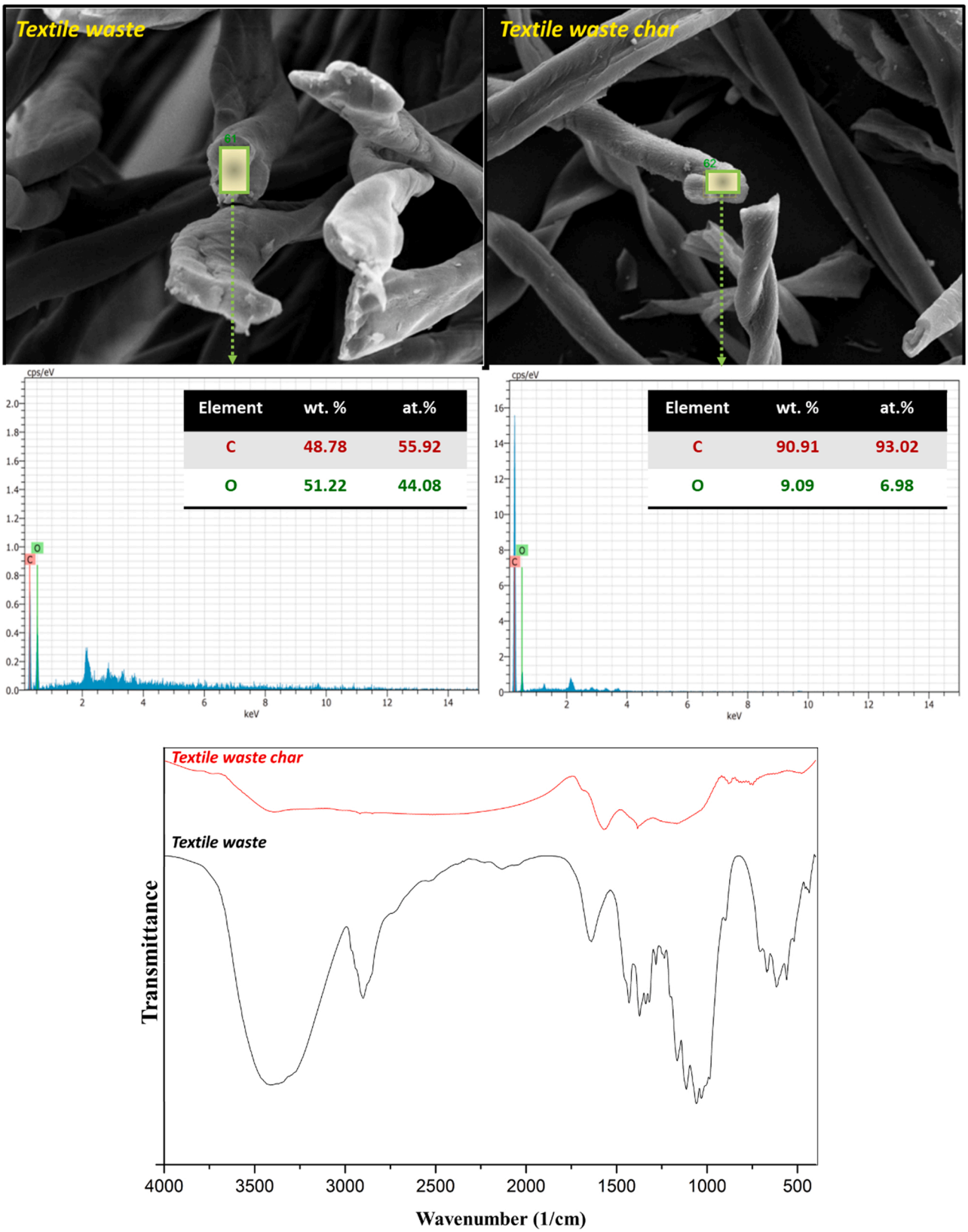

Fig. 7. Changes in morphology, elemental composition and functional groups during textile waste pyrolysis based on SEM-EDX (4000X) and FT-IR analyses.

the samples before and after pyrolysis are displayed in Fig. 6. These are beneficial to characterize the shapes of char particles, as well as their elemental composition based on EDX analysis. It may be seen that carbonized fibers appeared after the release of volatile compounds from the structure. At the end of the main pyrolysis zone, the fibrous particle size decreased, and the micro-fibrous structure was retained. The distinction in the surface morphology and thinning of the fibrous samples was caused by pyrolytic decomposition reactions. During pyrolysis,

Table 3
Thermodynamic parameters for textile waste pyrolysis.

α	ΔH (kj/mol)	ΔG (kj/mol)	ΔS (j/mol)
0.10	186.5	191.7	-8.4
0.15	199.7	199.0	1.1
0.20	194.4	196.1	-2.8
0.25	192.4	195.0	-4.3
0.30	194.5	196.2	-2.8
0.35	194.3	196.1	-2.9
0.40	194.2	196.1	-3.1
0.45	193.9	196.0	-3.3
0.50	193.8	195.9	-3.4
0.55	185.6	191.4	-9.3
0.60	183.2	190.0	-11.1
0.65	182.5	189.6	-11.7
0.70	171.0	183.3	-20.0
0.75	169.3	182.4	-21.3
0.80	161.2	177.9	-27.2
0.85	159.8	177.1	-28.2
0.90	155.7	174.9	-31.3
$\bar{x}$	**183.1**	**189.9**	**-11.2**

$\bar{x}$: Average value.

a number of reactions such as dehydration, decarbonylation, and decarboxylation occurred, which altered the morphology. After pyrolytic decomposition, the fibrous surface was obviously rougher, and significant shrinking was observed. As an important fact, it should be emphasized that textile waste carbonaceous chars with a carbon content greater than 90 wt% are produced by applying a moderate temperature during pyrolysis. Since the textile waste char had a tubular-like structure, it may have served as an alternative reinforcement for composites which can substitute low strength general-purpose carbon fibers due to the enhancement of the carbon content. As seen in the presented micrographs of the char, fiber-like structures also had some irregular, twisted shapes due to the evolution of volatiles from the structure. Chowdhury and Sarkar [74] indicated that devolatilization during pyrolysis decreases cell wall thickness and increases the proportion of voids as was also observed in the micrographs. When volatile materials passed through, the structure shrank, and some surface cracks that alter the fibrous morphology occurred. This disintegrated, twisted surface morphology due to the diffusion of volatiles should be further investigated, and the production conditions of char residue should be optimized to utilize the chars as an alternative filler material. In order to achieve porous textures such as activated carbon fibers, the pyrolyzed chars may be further activated by physical and chemical activation methods. Also, the char yield and characteristics may be enhanced by altering pyrolysis conditions such as heating rate and temperature since carbonization is favorable using lower heating rates and higher temperatures. This enhancement on the quality of the chars is related with the elimination of the functional groups and increase in the quantity of conjugated ringed structures[75].

FT-IR spectroscopy was employed to study the functional groups of the char residue after pyrolysis. The surface functional groups were qualitatively identified and compared as seen in Fig. 7. In comparison to the as-received textile waste, some surface groups disappeared due to the cracking of the structure. Removal of hydroxyl, alkyl and ester groups are observable which may be attributed to primary and secondary reactions during active pyrolysis such as dehydration, decarboxylation, methylation, aromatization, and fragmentation.

3.6. Thermodynamic analysis

Thermodynamic parameters were calculated according to the pre-exponential factor and the activation energy values that were determined using Friedman iso-conversional method. The variations in ΔH, ΔG, and ΔS with different conversion degrees are given in Table 3. According to the results, the change of ΔH is in line with the trend in activation energy. In a chemical process, the ΔH value indicates the energy difference between the products and reactants. For textile waste pyrolysis, ΔH values at all the conversion degree were positive, implying that the reaction was an endothermic process. Moreover, it is known that low ΔH values are favorable for the active complex formation, and show that products are easily formed when less energy is added. It's worth noting that modest differences between activation energy and ΔH (which is less than about 5 kJ/mol) suggest favorable conditions for the formation of activated complex due to the low potential barrier between the molecules of the samples [76]. The mean value of ΔH was 183.1 kJ/mol, which is found to be close to the mean value of the activation energy. The difference in activation energy ΔH at each conversion degree was also found to be close, which elucidates the progress of pyrolysis and the formation of products. On the other hand, another thermodynamic parameter, ΔG, represents the increase in total energy of the system with the activating complex formation. The higher value of the ΔG shows that the more energy the system must absorb throughout the reaction, whereas the lower the ΔG indicates the less energy is required for the formation of the products [76,77]. The ΔG values obtained for the pyrolysis of textile waste were in between 174.9 and 199.0 kJ/mol with an average value of 189.9 kj/mol. The numerical values of ΔG during active pyrolysis zone imply that the reactions were energetically endergonic and unfavorable. Therefore, non-spontaneous processes were driven throughout the thermal decomposition range. When it comes to the state function that depicts the degree of disorder of a system as ΔS, the lowest value of the ΔS was estimated at a conversion degree of 0.9 as − 31.3 j/mol.K. In the case of a higher ΔS value, the system is farther away from the thermodynamic equilibrium state which in turn shows the shorter the time required to form the activated complex [78]. Moreover, a higher ΔS showed that the system had not yet reached equilibrium, and the reaction rate would be faster if the reaction time was reduced. Negative ΔS values after the initiation stage of pyrolytic degradation imply that the product's degree of disorder is lower than the reactant's. The value of ΔS during pyrolysis of textile waste decreases with increasing conversion except the initial step, implying a slower reaction to form active complexes and therefore a longer reaction time.

4. Conclusions

As given in the kinetic results, the value of average activation energy was 188.2 kJ/mol, and the mean pre-exponential factor value was 3.22×10^{13} s^{-1} using Friedman method. When different kinetic methods were utilized, they were found compatible with Friedman's. In addition to thermokinetic study of textile wastes, thermodynamics of the process is analyzed. The variations in ΔH, ΔG, and ΔS with different conversion degree was estimated to determine favorability and status of the resultant products during pyrolytic degradation. Comparative online FT-IR and MS analysis, which was carried out simultaneously with TGA, confirmed the evolution of H_2O, CO_2, and CH_4, and the evolution profiles of these molecules were monitored. Moreover, the char residue was analyzed via SEM-EDX and ex-situ FT-IR. These results can be used as a baseline kinetic modeling benchmark large-scale pyrolysis simulation of textile industrial wastes. With efficiently developed feasible pyrolysis systems, these waste textile streams can be converted into favorable solid, liquid, and gaseous products with added value along with energy to promote awareness regarding waste management and circular economy.

CRediT authorship contribution statement

Gamzenur Özsin: Conceptualization, Methodology, Writing. **Ayşe Eren Pütün:** Supervision, Editing.

Declaration of Competing Interest

The authors declare that they have no known competing financial

interests or personal relationships that could have appeared to influence the work reported in this paper.

Acknowledgements

The authors would like to thank Carbon Materials Processing Group of Eskişehir Technical University for carrying out the TGA/MS/FT-IR analyses.

References

[1] M. Nelles, A. Schüch, G. Morscheck, Biogenious waste to energy–challenges and solutions, J. Sustain. Energy Environ. 61 (57) (2011).
[2] S. Nanda, F. Berruti, Municipal solid waste management and landfilling technologies: a review, Environ. Chem. Lett. 19 (2) (2021) 1433–1456.
[3] Y. Kobayashi, T.M. Ismail, T. Kobori, L. Ding, K. Yoshikawa, K. Araki, K. Kanazawa, F. Takahashi, Experimental investigation on the effect of electron injection into air for thermal decomposition of solid waste, Appl. Energy 295 (2021), 116999.
[4] H. Nan, L. Zhao, F. Yang, Y. Liu, Z. Xiao, X. Cao, H. Qiu, Different alkaline minerals interacted with biomass carbon during pyrolysis: Which one improved biochar carbon sequestration? J. Clean. Prod. 255 (2020), 120162.
[5] D. Reinhart, S.C. Bolyard, N. Berge, Grand Challenges–Management of municipal solid waste Elsevier 2016.
[6] M. Materazzi, A. Holt, Experimental analysis and preliminary assessment of an integrated thermochemical process for production of low-molecular weight biofuels from municipal solid waste (MSW), Renew. Energy 143 (2019) 663–678.
[7] S. Zuo, Z. Xiao, J. Yang, Evolution of gaseous products from biomass pyrolysis in the presence of phosphoric acid, J. Anal. Appl. Pyrolysis 95 (2012) 236–240.
[8] Y.-M. Kim, T.U. Han, B. Lee, A. Watanabe, N. Teramae, J.-H. Kim, Y.-K. Park, H. Park, S. Kim, Analytical pyrolysis reaction characteristics of Porphyra tenera, Algal Res. 32 (2018) 60–69.
[9] Z. Han, J. Li, T. Gu, B. Yan, G. Chen, The synergistic effects of polyvinyl chloride and biomass during combustible solid waste pyrolysis: Experimental investigation and modeling, Energy Convers. Manag. 222 (2020), 113237.
[10] Y. Xia, Y. Tang, K. Shih, B. Li, Enhanced phosphorus availability and heavy metal removal by chlorination during sewage sludge pyrolysis, J. Hazard. Mater. 382 (2020), 121110.
[11] A. Al-Rumaihi, P. Parthasarathy, A. Fernandez, T. Al-Ansari, H.R. Mackey, R. Rodriguez, G. Mazza, G. McKay, Thermal degradation characteristics and kinetic study of camel manure pyrolysis, J. Environ. Chem. Eng. (2021), 106071.
[12] J. Milovanović, R. Luque, R. Tschentscher, A.A. Romero, H. Li, K. Shih, N. Rajić, Study on the pyrolysis products of two different hardwood lignins in the presence of NiO contained-zeolites, Biomass Bioenergy 103 (2017) 29–34.
[13] H. Stančin, M. Šafář, J. Růžičková, H. Mikulčić, H. Raclavská, X. Wang, N. Duić, Co-pyrolysis and synergistic effect analysis of biomass sawdust and polystyrene mixtures for production of high-quality bio-oils, Process Saf. Environ. Prot. 145 (2021) 1–11.
[14] H.C. Ong, W.-H. Chen, A. Farooq, Y.Y. Gan, K.T. Lee, V. Ashokkumar, Catalytic thermochemical conversion of biomass for biofuel production: A comprehensive review, Renew. Sustain. Energy Rev. 113 (2019), 109266.
[15] W. Gu, J. Guo, J. Bai, B. Dong, J. Hu, X. Zhuang, C. Zhang, K. Shih, Co-pyrolysis of sewage sludge and Ca (H2PO4) 2: heavy metal stabilization, mechanism, and toxic leaching, J. Environ. Manag. 305 (2022), 114292.
[16] H. Hassan, B. Hameed, J. Lim, Co-pyrolysis of sugarcane bagasse and waste high-density polyethylene: Synergistic effect and product distributions, Energy 191 (2020), 116545.
[17] A. Veksha, A. Giannis, V.W.-C. Chang, Conversion of non-condensable pyrolysis gases from plastics into carbon nanomaterials: effects of feedstock and temperature, J. Anal. Appl. Pyrolysis 124 (2017) 16–24.
[18] Q. Jin, X. Wang, S. Li, H. Mikulčić, T. Bešenić, S. Deng, M. Vujanović, H. Tan, B.M. Kumfer, Synergistic effects during co-pyrolysis of biomass and plastic: Gas, tar, soot, char products and thermogravimetric study, Journal of the Energy Institute (2017).
[19] Y. Liu, C. Ran, A.A. Siyal, Y. Song, Z. Jiang, J. Dai, P. Chtaeva, J. Fu, W. Ao, Z. Deng, Comparative study for fluidized bed pyrolysis of textile dyeing sludge and municipal sewage sludge, J. Hazard. Mater. 396 (2020), 122619.
[20] Q.-V. Bach, W.-H. Chen, C.F. Eng, C.-W. Wang, K.-C. Liang, J.-Y. Kuo, Pyrolysis characteristics and non-isothermal torrefaction kinetics of industrial solid wastes, Fuel 251 (2019) 118–125.
[21] J. Li, F. Zheng, Q. Li, M.Z. Farooq, F. Lin, D. Yuan, B. Yan, Y. Song, G. Chen, Effects of inherent minerals on oily sludge pyrolysis: Kinetics, products, and secondary pollutants, Chem. Eng. J. 431 (2022), 133218.
[22] G. Yu, D. Chen, U. Arena, Z. Huang, X. Dai, Reforming sewage sludge pyrolysis volatile with Fe-embedded char: minimization of liquid product yield, Waste Manag. 73 (2018) 464–475.
[23] W.C. Udayanga, A. Veksha, A. Giannis, G. Lisak, T.-T. Lim, Effects of sewage sludge organic and inorganic constituents on the properties of pyrolysis products, Energy Convers. Manag. 196 (2019) 1410–1419.
[24] Z. Ni, H. Bi, C. Jiang, J. Tian, H. Sun, W. Zhou, Q. Lin, Research on the co-pyrolysis of coal gangue and coffee industry residue based on machine language: Interaction, kinetics, and thermodynamics, Sci. Total Environ. 804 (2022), 150217.
[25] G. Özsin, E. Apaydın-Varol, M. Kılıç, A.E. Pütün, E. Pütün, Pyrolysis of petroleum sludge under non-isothermal conditions: thermal decomposition behavior, kinetics, thermodynamics, and evolved gas analysis, Fuel 300 (2021), 120980.
[26] R. Chen, Q. Li, Y. Zhang, X. Xu, D. Zhang, Pyrolysis kinetics and mechanism of typical industrial non-tyre rubber wastes by peak-differentiating analysis and multi kinetics methods, Fuel 235 (2019) 1224–1237.
[27] N. Pensupa, S.-Y. Leu, Y. Hu, C. Du, H. Liu, H. Jing, H. Wang, C.S.K. Lin, Recent trends in sustainable textile waste recycling methods: current situation and future prospects. Chemistry and Chemical Technologies in Waste Valorization, Springer, 2017, pp. 189–228.
[28] A. Lopatina, I. Anugwom, H. Blot, Á.S. Conde, M. Mänttäri, M. Kallioinen, Re-use of waste cotton textile as an ultrafiltration membrane, J. Environ. Chem. Eng. 9 (4) (2021), 105705.
[29] G. Xia, W. Han, Z. Xu, J. Zhang, F. Kong, J. Zhang, X. Zhang, F. Jia, Complete recycling and valorization of waste textiles for value-added transparent films via an ionic liquid, J. Environ. Chem. Eng. 9 (5) (2021), 106182.
[30] K. Shirvanimoghaddam, B. Motamed, S. Ramakrishna, M. Naebe, Death by waste: Fashion and textile circular economy case, Sci. Total Environ. 718 (2020), 137317.
[31] V. Lahtela, A. Kumar, T. Kärki, The impact of textile waste on the features of high-density polyethylene (HDPE) composites, Urban Sci. 5 (3) (2021) 59.
[32] M.-P. Todor, I. Kiss, V.G. Cioata, Development of fabric-reinforced polymer matrix composites using bio-based components from post-consumer textile waste, Mater. Today.: Proc. 45 (2021) 4150–4156.
[33] D. Kwon, S. Yi, S. Jung, E.E. Kwon, Valorization of synthetic textile waste using CO_2 as a raw material in the catalytic pyrolysis process, Environ. Pollut. 268 (2020), 115916.
[34] Y. Wu, C. Wen, X. Chen, G. Jiang, G. Liu, D. Liu, Catalytic pyrolysis and gasification of waste textile under carbon dioxide atmosphere with composite Zn-Fe catalyst, Fuel Process. Technol. 166 (2017) 115–123.
[35] P.T. Williams, A.R. Reed, High grade activated carbon matting derived from the chemical activation and pyrolysis of natural fibre textile waste, J. Anal. Appl. Pyrolysis 71 (2) (2004) 971–986.
[36] Y. Wei, H. Liu, S. Liu, M. Zhang, Y. Shi, J. Zhang, L. Zhang, C. Gong, Waste cotton-derived magnetic porous carbon for high-efficiency microwave absorption, Compos. Commun. 9 (2018) 70–75.
[37] Y.P. Rago, D. Surroop, R. Mohee, Torrefaction of textile waste for production of energy-dense biochar using mass loss as a synthetic indicator, J. Environ. Chem. Eng. 6 (1) (2018) 811–822.
[38] S. Yousef, J. Eimontas, N. Striūgas, M. Tatariants, M.A. Abdelnaby, S. Tuckute, L. Kliucininkas, A sustainable bioenergy conversion strategy for textile waste with self-catalysts using mini-pyrolysis plant, Energy Convers. Manag. 196 (2019) 688–704.
[39] M.A. Nahil, P.T. Williams, Activated carbons from acrylic textile waste, J. Anal. Appl. Pyrolysis 89 (1) (2010) 51–59.
[40] J. Zheng, Q. Zhao, Z. Ye, Preparation and characterization of activated carbon fiber (ACF) from cotton woven waste, Appl. Surf. Sci. 299 (2014) 86–91.
[41] A. Fernandez, A. Saffe, R. Pereyra, G. Mazza, R. Rodriguez, Kinetic study of regional agro-industrial wastes pyrolysis using non-isothermal TGA analysis, Appl. Therm. Eng. 106 (2016) 1157–1164.
[42] S. Gerassimidou, C.A. Velis, P.T. Williams, D. Komilis, Characterisation and composition identification of waste-derived fuels obtained from municipal solid waste using thermogravimetry: a review, Waste Manag. Res. 38 (9) (2020) 942–965.
[43] T. Yasmin, A. Asghar, M.S. Ahmad, M.A. Mehmood, M. Nawaz, Biorefinery potential of Typha domingensis biomass to produce bioenergy and biochemicals assessed through pyrolysis, thermogravimetry, and TG-FTIR-GCMS-based study, Biomass Convers. Biorefin. (2021) 1–13.
[44] G. Özsin, M. Kılıç, E. Apaydin-Varol, A.E. Pütün, E. Pütün, A thermo-kinetic study on co-pyrolysis of oil shale and polyethylene terephthalate using TGA/FT-IR, Korean J. Chem. Eng. (2020) 1–11.
[45] B.B. Uzun, A.E. Pütün, E. Pütün, Fast pyrolysis of soybean cake: product yields and compositions, Bioresour. Technol. 97 (4) (2006) 569–576.
[46] G. Özsin, A.E. Pütün, A comparative study on co-pyrolysis of lignocellulosic biomass with polyethylene terephthalate, polystyrene, and polyvinyl chloride: synergistic effects and product characteristics, J. Clean. Prod. 205 (2018) 1127–1138.
[47] W. Kuang, M. Lu, I. Yeboah, G. Qian, X. Duan, J. Yang, D. Chen, X. Zhou, A comprehensive kinetics study on non-isothermal pyrolysis of kerogen from Green River oil shale, Chem. Eng. J. 377 (2019), 120275.
[48] C. Doyle, Estimating isothermal life from thermogravimetric data, J. Appl. Polym. Sci. 6 (24) (1962) 639–642.
[49] R. Agrawal, M. Sivasubramanian, Integral approximations for nonisothermal kinetics, AIChE J. 33 (7) (1987) 1212–1214.
[50] G.I. Senum, R. Yang, Rational approximations of the integral of the Arrhenius function, J. Therm. Anal. 11 (3) (1977) 445–447.
[51] H. Eyring, The activated complex in chemical reactions, J. Chem. Phys. 3 (2) (1935) 107–115.
[52] B. Boonchom, Kinetics and thermodynamic properties of the thermal decomposition of manganese dihydrogenphosphate dihydrate, J. Chem. Eng. Data 53 (7) (2008) 1533–1538.
[53] B. Singh, P. Kumar, Physicochemical characteristics of hazardous sludge from effluent treatment plant of petroleum refinery as feedstock for thermochemical processes, J. Environ. Chem. Eng. 8 (4) (2020), 103817.
[54] A. Hanoğlu, A. Çay, J. Yanık, Production of biochars from textile fibres through torrefaction and their characterisation, Energy 166 (2019) 664–673.

[55] S. Ceylan, Y. Topçu, Pyrolysis kinetics of hazelnut husk using thermogravimetric analysis, Bioresour. Technol. 156 (2014) 182–188.
[56] T. Xu, F. Xu, Z. Hu, Z. Chen, B. Xiao, Non-isothermal kinetics of biomass-pyrolysis-derived-tar (BPDT) thermal decomposition via thermogravimetric analysis, Energy Convers. Manag. 138 (2017) 452–460.
[57] Y. Qu, A. Li, D. Wang, L. Zhang, G. Ji, Kinetic study of the effect of in-situ mineral solids on pyrolysis process of oil sludge, Chem. Eng. J. 374 (2019) 338–346.
[58] J.J. Krishna, S.S. Damir, R. Vinu, Pyrolysis of electronic waste and their mixtures: kinetic and pyrolysate composition studies, J. Environ. Chem. Eng. 9 (4) (2021), 105382.
[59] G. Lopez, J. Alvarez, M. Amutio, B. Hooshdaran, M. Cortazar, M. Haghshenasfard, S.H. Hosseini, M. Olazar, Kinetic modeling and experimental validation of biomass fast pyrolysis in a conical spouted bed reactor, Chem. Eng. J. 373 (2019) 677–686.
[60] D.I. Aslan, P. Parthasarathy, J.L. Goldfarb, S. Ceylan, Pyrolysis reaction models of waste tires: application of Master-Plots method for energy conversion via devolatilization, Waste Manag. 68 (2017) 405–411.
[61] B. Janković, N. Manić, V. Dodevski, Pyrolysis kinetics of Poplar fluff bio-char produced at high carbonization temperature: A mechanistic study and isothermal life-time prediction, Fuel 296 (2021), 120637.
[62] H. Liu, G. Xu, G. Li, Pyrolysis characteristic and kinetic analysis of sewage sludge using model-free and master plots methods, Process Saf. Environ. Prot. 149 (2021) 48–55.
[63] C.I. Akor, A.I. Osman, C. Farrell, C.S. McCallum, W.J. Doran, K. Morgan, J. Harrison, P.J. Walsh, G.N. Sheldrake, Thermokinetic study of residual solid digestate from anaerobic digestion, Chem. Eng. J. 406 (2021), 127039.
[64] D. Hungwe, S. Ullah, P. Kilpeläinen, S. Theppitak, L. Ding, F. Takahashi, Potassium demineralization of coconut fiber via combined hydrothermal treatment and washing: Effect on pyrolysis kinetics, mechanisms, and bio-oil composition, Biomass Bioenergy 152 (2021), 106194.
[65] H. Tian, Q. Hu, J. Wang, L. Liu, Y. Yang, A.V. Bridgwater, Steam gasification of Miscanthus derived char: the reaction kinetics and reactivity with correlation to the material composition and microstructure, Energy Convers. Manag. 219 (2020), 113026.
[66] H.H. Muigai, B.J. Choudhury, P. Kalita, V.S. Moholkar, Physico–chemical characterization and pyrolysis kinetics of Eichhornia crassipes, Thevetia peruviana, and Saccharum officinarum, Fuel 289 (2021), 119949.
[67] E. Torres-García, L. Ramírez-Verduzco, J. Aburto, Pyrolytic degradation of peanut shell: Activation energy dependence on the conversion, Waste Manag. 106 (2020) 203–212.
[68] G. Özsin, K.B. Dermenci, S. Turan, Thermokinetic and thermodynamics of Pechini derived Li 7− 3x Al x La 3 Zr 2 O 12 (X= 0.0–0.2) xerogel decomposition under oxidative conditions, J. Therm. Anal. Calorim. (2021) 1–16.
[69] L. Hu, X.-Y. Wei, X.-H. Guo, H.-P. Lv, G.-H. Wang, Investigation on the kinetic behavior, thermodynamic and volatile products analysis of chili straw waste pyrolysis, J. Environ. Chem. Eng. 9 (5) (2021), 105859.
[70] M.A. Mehmood, M.S. Ahmad, Q. Liu, C.-G. Liu, M.H. Tahir, A.A. Aloqbi, N. I. Tarbiah, H.M. Alsufiani, M. Gull, Helianthus tuberosus as a promising feedstock for bioenergy and chemicals appraised through pyrolysis, kinetics, and TG-FTIR-MS based study, Energy Convers. Manag. 194 (2019) 37–45.
[71] D. Che, L. Wang, H. Liu, B. Sun, S. Guo, Effects of lipids on sludge and chlorella protein pyrolysis by thermogravimetry Fourier transform infrared spectrometry, J. Environ. Chem. Eng. 10 (1) (2022), 107011.
[72] R. Zhao, L. Liu, Y. Bi, L. Tian, X. Wang, Determination of pyrolysis characteristics and thermo-kinetics to assess the bioenergy potential of Phragmites communis, Energy Convers. Manag. 207 (2020), 112510.
[73] J. Ordonez-Loza, F. Chejne, A.G.A. Jameel, S. Telalovic, A.A. Arrieta, S.M. Sarathy, An investigation into the pyrolysis and oxidation of bio-oil from sugarcane bagasse: Kinetics and evolved gases using TGA-FTIR, J. Environ. Chem. Eng. (2021), 106144.
[74] R. Chowdhury, A. Sarkar, Reaction kinetics and product distribution of slow pyrolysis of Indian textile wastes, Int. J. Chem. React. Eng. 10 (1) (2012).
[75] C. Li, C. Zhang, G. Gao, M. Gholizadeh, S. Zhang, L. Xu, L. Zhang, Q. Li, X. Hu, Interaction of the volatiles from co-pyrolysis of pig manure with cellulose/glucose and their effects on char properties, J. Environ. Chem. Eng. 8 (6) (2020), 104583.
[76] H. Peng, P. Li, Q. Yang, Investigation on the reaction kinetics, thermodynamics and synergistic effects in co-pyrolysis of polyester and viscose fibers, React. Kinet. Mech. Catal. (2022) 1–25.
[77] S. Singh, J.P. Chakraborty, M.K. Mondal, Intrinsic kinetics, thermodynamic parameters and reaction mechanism of non-isothermal degradation of torrefied Acacia nilotica using isoconversional methods, Fuel 259 (2020), 116263.
[78] J. Ma, H. Luo, Y. Li, Z. Liu, D. Li, C. Gai, W. Jiao, Pyrolysis kinetics and thermodynamic parameters of the hydrochars derived from co-hydrothermal carbonization of sawdust and sewage sludge using thermogravimetric analysis, Bioresour. Technol. 282 (2019) 133–141.